Monthly Notices of the ROYAL ASTRONOMICAL SOCIETY

MNRAS **517,** L81–L85 (2022) https://doi.org/10.1093/mnrasl/slac114

LOFAR discovery of rare large FR I jets in the low-luminosity radio galaxy NGC 5322

Amitesh Omar ★

Aryabhatta Research Institute of Observational Sciences, Manora Peak, Nainital, 263001, India

Accepted 2022 September 21. Received 2022 September 21; in original form 2022 June 29

ABSTRACT

The discovery of faint Fanaroff–Riley type I (FR I) radio jets in the elliptical galaxy NGC 5322 is reported here using the 144-MHz image from Data Release 2 of the Low-Frequency Array (LOFAR) Two-metre Sky Survey (LoTSS). The jets have an angular extent of ∼40 arcmin or a projected physical extent of ∼360 kpc. The faint jets remain well collimated and disappear in the intergalactic medium, without any detected hotspots or radio lobes. The relatively brighter jets, previously detected only up to the ∼21 kpc extent at higher frequencies, are within the optical extent of the galaxy. The jets become faint abruptly outside, where detection is made only in the LOFAR image. The total radio luminosity of the galaxy at 144 MHz is estimated to be $(3.7 \pm 0.4) \times 10^{22}$ W Hz^{-1}. The 144-MHz radio luminosity of the faint jets outside the optical extent is estimated to be $(7.1 \pm 2.0) \times 10^{21}$ W Hz^{-1}. The size of the jets is exceptionally large for the galaxy's low radio luminosity, when compared with other radio galaxies. It makes NGC 5322 a rare radio galaxy, previously not detected in other radio surveys. A combined effect of stellar core depletion and low-density environment around the jets, which results in a weak entrainment of the material surrounding the jets, could be responsible for its large size despite a low radio luminosity.

Key words: galaxies: active – intergalactic medium – galaxies: jets – galaxies: nuclei – radio continuum: galaxies.

1 INTRODUCTION

NGC 5322 is an optically bright ($m_r \sim 10.3$ mag; $M_r \sim -22.2$ mag), nearby (with a distance of ∼31 Mpc and scale 1 arcmin ∼ 9 kpc; Tonry et al. 2001), elliptical (E3−4; de Vaucouleurs et al. 1991) radio galaxy of Low Ionization Nuclear Emission Region (LINER) type (Baldi & Capetti 2009). It was detected in early radio interferometric surveys using the Westerbork Synthesis Radio Telescope (WSRT) and the Very Large Array (VLA) at frequencies of 1.4 GHz and 5.0 GHz (Sramek 1975; Hummel 1980; Hummel, van der Hulst & Dickey 1984). These observations revealed two classical bipolar radio jets on kpc-scales and a core. The radio jets with an extent of ∼2.3 arcmin (∼21 kpc) at a position angle (PA) of nearly −7° in the 1.4-GHz WSRT image, at a resolution of 15 × 13 arcsec^2 and detection sensitivity of 0.5 mJy beam^{-1}, were found to be completely embedded within the optical extent of the galaxy (Feretti et al. 1984). Nagar, Falke & Wilson (2005) identified a core–jet morphology in NGC 5322 using Very Large Baseline Array (VLBA) observations. Dullo et al. (2018) presented high angular resolution images of NGC 5322 at 1.5 GHz using the e-MERLIN array and optical observations using the *Hubble Space Telescope* (*HST*). The *HST* image revealed an edge-on nuclear dust disc, aligned with the major axis of the galaxy and nearly perpendicular to the parsec-scale radio jets detected in the e-MERLIN image.

The 1.4-GHz flux of NGC 5322 in the NRAO VLA Sky Survey (NVSS; Condon et al. 1998) is 78 ± 3 mJy, which is in good agreement with the earlier 1.4-GHz WSRT estimate of 84 ± 4 mJy by Feretti et al. (1984). The 1.4-GHz image from the Faint Images of the Radio Sky at Twenty-Centimeters (FIRST) survey (Becker, White & Helfand 1995) shows a core–jet morphology at 5-arcsec resolution. The galaxy is also detected in images at 325 MHz from the Westerbork Northern Sky Survey (WENSS; Rengelink et al. 1997), at 150 MHz from the TIFR GMRT Sky Survey (TGSS; Intema et al. 2017) using the Giant Metrewave Radio Telescope (GMRT), and at 74 MHz from the VLA Low-Frequency Sky Survey Redux (VLSSr; Lane et al. 2014). The source is slightly resolved in the NVSS and TGSS images and unresolved in the VLSSr image. The radio flux densities of NGC 5322 from different radio surveys up to a frequency of 1.4 GHz are provided in Table 1.

The radio emission from NGC 5322 was examined in the recently released Low-Frequency Array (LOFAR; van Haarlem et al. 2013) Two-metre Sky Survey (LoTSS) Data Release 2 (DR2) images at 144 MHz (Shimwell et al. 2022). The LoTSS is being carried out with the LOFAR (the Netherlands), using wide-bandwidth (120−168 MHz) high-band antennas. The calibrated and de-convolved images are provided in the LoTSS image archives. These images have high fidelity and are capable of detecting extended radio emission. The flux density scale in the LoTSS DR2 survey is expected to be accurate within ±10 per cent. NGC 5322 is detected in the LoTSS data mosaic P207+60 with an angular offset of 0.°27 from the mosaic centre.

Capetti et al. (2022) published an image of NGC 5322 using the LoTSS DR2 data, but their image only covers the inner bright part of the jets and they did not mention the much larger extent of the jets very clearly seen in the low-resolution version of the LoTSS DR2 images. This large-scale radio emission is also not detected in the 235-MHz and 610-MHz GMRT images presented by Kolokythas

★ E-mail: aomar@aries.res.in

Table 1. Radio flux of NGC 5322.

Frequency (MHz)	Total flux (mJy)	LAS (arcsec)	rms (mJy beam^{-1})	Ref.
74	432 ± 51	1100	65	VLSSr
144	266 ± 27^{C} 36 ± 9^{N} 25 ± 8^{S}	2578	0.055	LoTSS
150	217 ± 22	4125	2.8	TGSS
235	135 ± 11	2620	0.7	GMRT
327	144 ± 6	1375	3.8	WENSS
610	106 ± 5	1010	0.05	GMRT
1400	78 ± 3	970	0.5	NVSS

Note. LAS denotes the largest angular scales that can be reliably detected in interferometric surveys. These are taken from Savini et al. (2017) for all the surveys except for TGSS/GMRT, in which they are estimated using the shortest baseline of 100 m in the GMRT. *C* indicates flux density for the bright jet portion within ±1.1 arcmin from the centre measured in this work. *N* and *S* indicate flux densities for northern and southern jets, respectively.

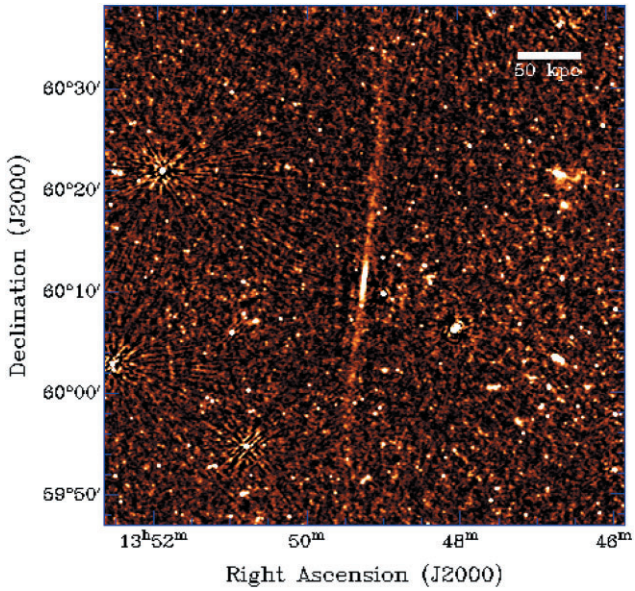

Figure 1. 144-MHz LoTSS image of NGC 5322. The image is taken from a high-resolution mosaic and later smoothed using a Gaussian kernel with a width of 7.5 × 7.5 arcsec^2. The rms in the raw image is 55 μJy beam^{-1} at an angular resolution of 6 × 6 arcsec^2.

et al. (2019), with rms values of 0.7 mJy beam^{-1} and 50 μJy beam^{-1}, respectively.

Here, we report on the detection of faint radio jets in NGC 5322 using the LoTSS image. We discuss the astrophysical scenarios for its origin. We have used the cosmological parameters $H_0 = 70$ km s^{-1} Mpc^{-1}, $\Omega_M = 0.3$ and a flat Universe to derive distances. The distance to NGC 5322 is taken here from the redshift-independent surface brightness fluctuation measurements (Tonry et al. 2001).

2 LOFAR RADIO MORPHOLOGY

Fig. 1 shows the 144-MHz high-resolution (6 × 6 arcsec^2) LoTSS image of NGC 5322. This image is smoothed using a Gaussian kernel (7.5 × 7.5 arcsec^2) to enhance diffuse radio emission. The image is contrast-adjusted on non-linear scales to reveal faint diffuse emission

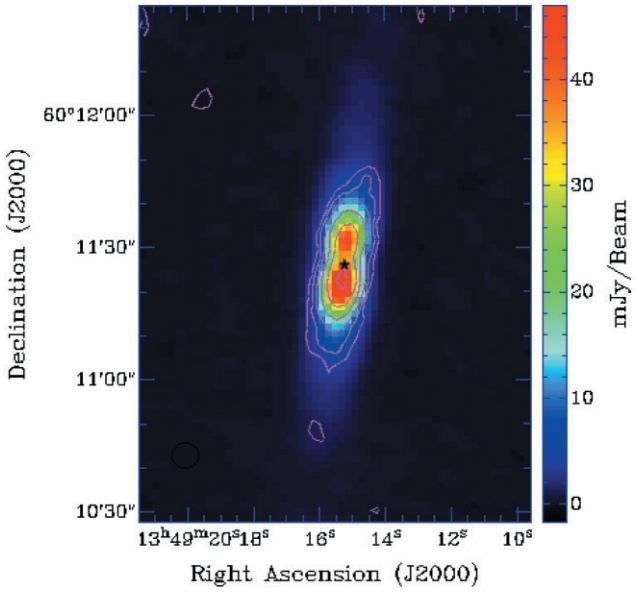

Figure 2. Contours from the 1.4-GHz FIRST image overlaid upon the 144-MHz LoTSS image of NGC 5322. The contour levels are 0.45 mJy beam^{-1} × (1, 2, 4, 8, 16, 32). The black star indicates the position of the optical nucleus.

in the presence of bright radio sources. Two classical jet-like features emanating from the galaxy are detected. The jets are bright within ±1 arcmin from the centre and afterwards become faint. The faint jet-like features on scales of tens of arcmin cannot be de-convolution errors as these errors have a different pattern, which can be seen around bright point sources in the image. The jets are nearly north–south (PA ∼ 8°) oriented and detected between the declinations 59° 52′ and 60° 32′. The jet emission appears fragmented on smaller scales; however, because of the poor signal-to-noise ratio, details cannot be quantified. The angular extent of the jets (∼40 arcmin) is close to the largest angular scale (LAS) that the LOFAR can possibly sample (see, e.g. Savini et al. 2017). Therefore, the true extents of the jets may be larger than that detected in the LoTSS image. The typical LAS values for different radio surveys are provided in Table 1.

The angular resolutions in the FIRST image and the LoTSS image are comparable. An overlay of the two images is shown in Fig. 2. The bright regions of NGC 5322 in the two images have very similar radio morphologies with identical locations for the brightest emission region. The southern jet appears to be brighter than the northern jet in the inner region. The jets detected in the 1.4-GHz WSRT image (Feretti et al. 1984) within ±1.1 arcmin from the centre are detected as bright jets in the 144-MHz LoTSS image, also with roughly similar extents. The faint jets on larger scales, detected in the LoTSS image, are not detected in any other radio survey. The total flux at 144 MHz is measured for the central bright portion of the jets over ±1.1 arcmin from the centre so that it can be compared with the measurements from past surveys. The average spectral index (α; where $S \propto \nu^{\alpha}$) of the bright jet (within ±1.1 arcmin) is estimated to be -0.67 ± 0.14 between 1.4 GHz and 144 MHz, using the flux values provided in Table 1. The radio emission is therefore of synchrotron origin, typical for radio galaxies. It was assumed here that all other radio surveys detected the bright jets, although as a result of poor angular resolution this is not verifiable in all the cases. We use 'faint jets' hereafter to refer to those detected in the LoTSS image only. The quoted errors in the flux density values at 144 MHz are estimated as a combination of rms in the summed region and a 10 per cent calibration error. The

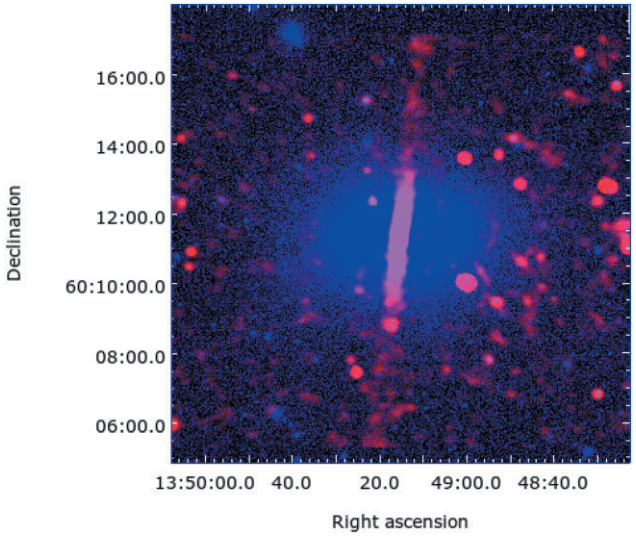

Figure 3. Colour overlays of the SDSS *i*-band image (blue) and the 144-MHz LoTSS image (red) highlighting the central bright emission region within the optical extent of NGC 5322.

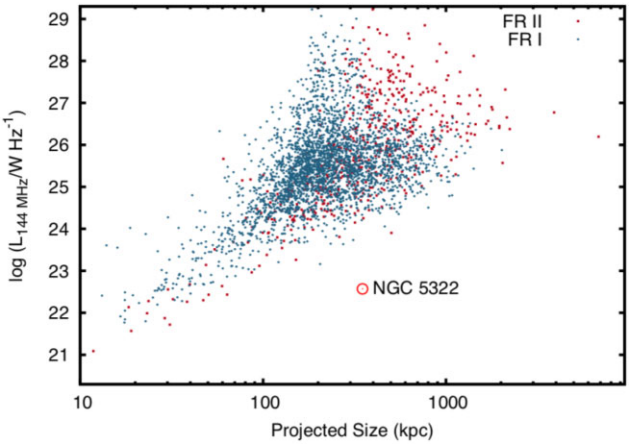

Figure 4. Location of NGC 5322 in the luminosity–size plot for FR I and FR II galaxies detected in the LoTSS DR1 and first made available in Mingo et al. (2019). The origins of redshifts are spectroscopic (wherever available) or else photometric. The luminosities are K-corrected with a spectral index of −1. The symbols are explained in the upper-right corner.

flux estimated from the 150-MHz TGSS image is marginally different from that in the 144-MHz LoTSS image, although the values agree within the flux calibration errors in the two surveys.

A colour overlay of the LoTSS image and the optical *i*-band image from the Sloan Digital Sky Survey (SDSS) is shown in Fig. 3. The jets seem to abruptly become faint after leaving the bright optical extent of the galaxy. The faint jets remain well collimated over a long distance and appear to diffuse out in outer regions before disappearing (see Fig. 1). The projected physical length of the jets is estimated to be ∼360 kpc. The northern faint jet (flux = 36 ± 9 mJy) appears relatively brighter than the southern faint jet (flux = 25 ± 8 mJy). The radio surface brightness of the faint jets in the LoTSS image varies between 1.4 and 2.5 μJy arcsec^{-2} in different regions. The faint jets are not detected in the TGSS because of the much higher rms in the TGSS, despite being sensitive to the LAS on slightly more than a degree. The faint jets are not detected in other surveys due to limitations arising from both rms and LAS sensitivities and the jets getting fainter at higher frequencies.

3 DISCUSSION

The 144-MHz radio morphology of NGC 5322 appears to be of the classical FR I type (see Fanaroff & Riley 1974) as the jets are edge-darkened. The 1.4-GHz radio luminosity using the NVSS flux is estimated to be $\sim 1 \times 10^{22}$ W Hz^{-1}, which makes NGC 5322 a low-luminosity radio galaxy. The 144-MHz radio luminosity of the large-scale faint radio jets outside the optical extent is estimated to be $(7.1 \pm 2.0) \times 10^{21}$ W Hz^{-1} and that of all radio emission at 144 MHz associated with NGC 5322 is estimated to be $(3.7 \pm 0.4) \times 10^{22}$ W Hz^{-1}. The projected end-to-end extent of the radio jets is ∼360 kpc. For the radio luminosity, this source size is exceptionally large, as can be seen from Fig. 4, where luminosities and sizes are plotted for FR I and FR II galaxies up to $z \sim 2$, detected in the LoTSS DR1, using data provided in Mingo et al. (2019) and Williams et al. (2019). It can be seen from Fig. 4 that for sources with sizes similar to that of NGC 5322, the typical radio luminosity of galaxies is more than one order of magnitude higher than that of NGC 5322. The same inference could also be drawn from an earlier luminosity–size plot made by An & Baan (2012) at 1.4 GHz. Therefore, NGC 5322 is a rare radio galaxy, detected for the first time to the best of our knowledge, having oversized radio jets with at least one order of magnitude lower radio luminosity than other radio galaxies. These large radio jets in NGC 5322 are detected for the first time, because of the unprecedented sensitivity of the LOFAR at low radio frequencies where radio jets become bright. Usually such long jets end in diffuse low-surface brightness lobes; however, such features are not detected in NGC 5322. Some nearby examples of collimated jets, which do not terminate in lobes, are found in NGC 2663 (Velović et al. 2022) and NGC 3665 (Capetti et al. 2022).

Other important features of the jets in NGC 5322 are its abrupt dimming outside the optical extent of the galaxy and its collimation on scales of 100 kpc. The jets in most radio galaxies almost always propagate at relativistic speeds. The emissivity of the jets is affected by various particle energy loss processes such as synchrotron emission, adiabatic expansion, and inverse-Compton scattering of cosmic microwave background photons (see, e.g. An & Baan 2012). The efficiency of different energy loss processes can vary across the length of the jet; for example, the synchrotron losses will dominate highly relativistic jets in high magnetic fields while the inverse-Compton loss will dominate at or near the outer ends of jets and lobes with low magnetic field strengths. The evolutions of jets and its magnetic field are complex and can depend on various parameters, such as central black hole (BH) properties (e.g. mass, spin, accretion), the initial jet power, and the physical conditions of the interstellar medium (ISM) and intergalactic medium (IGM) surrounding the jets (see reviews by Hardcastle & Croston 2020 and Saikia 2022).

The jets in the FR I radio galaxies are modelled as turbulent decelerating flows. In a classical picture, low-power FR I jets slow down, become subrelativistic, de-collimate and disperse into a wider jet or diffuse radio lobes beyond the distance of a few tens of kpc from the parent galaxy (see, e.g. Laing & Bridle 2002). However, more powerful FR II jets remain well collimated and are able to create bright hotspots and radio lobes up to a distance of several hundreds of kpc from the galaxy. As is evident from Fig. 4, this classical FR I/FR II dichotomy in terms of the jet power has now virtually disappeared and jets with different powers can be represented by both FR I and FR II morphologies. The analysis presented in Mingo et al. (2019) supports a widely discussed connection between the jet morphology and its inner environment (see, e.g. Gopal-Krishna & Wiita 2000).

The entrainment of the thermal material (e.g. ISM created in stellar winds, dense molecular clouds, and atomic gas, etc.) in the vicinity of jets can effectively slow down the jets (see, e.g. Laing & Bridle 2002) and may also be responsible for magnetic field evolution and particle (re)acceleration (e.g. Young et al. 2011). This entrainment process will be less effective in high-power jets where a laminar flow can be maintained over large distances. In order to understand the 360 kpc well-collimated FR I jets in NGC 5322, some important properties of the galaxy and its environment are summarized below. Although the FR I and FR II nomenclature in the present context may not be important, we still emphasize 'FR I' jets in NGC 5322 as neither FR I nor FR II radio sources were previously detected in the region in the luminosity–size diagram where NGC 5322 is found to be located.

NGC 5322 is the brightest member of a galaxy group that has a velocity dispersion of $\sim$169 km s^{-1} with 21 members (Makarov & Karachentsev 2011). In a study of several galaxy groups using *XMM–Newton*, Finoguenov et al. (2006) found that NGC 5322 is an X-ray faint (log $L_{\rm X} = 40.41 \pm 0.38$ erg s^{-1}; Mulchaey et al. 2003) group with exceptionally low thermal pressure in the X-ray emitting gas in the inner region. As the X-ray emission was detected only in close proximity to the central BH, it was suggested that it was coming from the ISM within the galaxy and not any infalling matter on cluster-wide scales associated with a cosmological structure formation. Therefore, the IGM surrounding NGC 5322 is likely to be of very low density. We found NGC 5322 to be well located in the fundamental plane of the BH activity, described by Merloni, Heinz & di Matteo (2003) as a relation between the X-ray luminosity, BH mass, and 5-GHz radio luminosity, within its scatter, using the X-ray luminosity (log $L_{\rm X}$/erg s^{-1} $= 40.41 \pm 0.38$; Mulchaey et al. 2003), the BH mass (log $M_{\rm BH}/{\rm M}_{\odot} = 8.41 \pm 0.40$; Dullo et al. 2018), and the 5-GHz luminosity (log $L_{5\,{\rm GHz}}$/erg s^{-1} $= 38.3 \pm 0.08$), using the 4.8-GHz flux as 47 ± 7 mJy from Gregory & Condon (1991) for NGC 5322. Therefore, the BH activities in NGC 5322 appear to be similar to other radio galaxies in terms of the central engine properties and the jet power.

NGC 5322 is also a core-depleted galaxy with a large deficit of stellar mass in the core (Dullo et al. 2018). Such cores can result from dry mergers of galaxies. NGC 5322 lacks a rich ISM, as evidenced from the non-detection of both molecular hydrogen (Young et al. 2011) and neutral hydrogen emission (Hibbard & Sansom 2003; Serra et al. 2012). Only narrow neutral hydrogen absorption has been detected (Serra et al. 2012). This absorption is likely to be originating in the edge-on dusty kpc-scale disc detected in the *HST* image.

With the aforementioned inferred properties of the ISM and IGM surrounding the radio jets in NGC 5322, we could speculate about the following astrophysical situation for exceptionally large-scale jets in NGC 5322. The jets in NGC 5322 are most likely undergoing weak entrainment from the ISM within the galaxy and even much weaker entrainment from the IGM outside the galaxy. The slow-down process of the jets on parsec-scale could also be very weak due to a large deficit of the stellar material in the environment of the inner jets. The likely scenario for the large collimated jets in NGC 5322 therefore appears to be a lack of dense material (stars or gas) near the core and a low-density of the ISM and IGM surrounding the jets throughout its progression. This result strengthens the views presented in some earlier studies (e.g. Mingo et al. 2019; Gopal-Krishna & Wiita 2000) where the FR dichotomy is explained based upon some interaction of jets with the medium external to the central engine. Under such a theoretical scenario where the brightness evolution (re-acceleration) and the collimation of jets on large scales are governed entirely by some entrainment of material, the jets may remain well collimated over long distances due to a lack of strong external instabilities and may also become faint due to a lack of particle (re)acceleration.

4 SUMMARY

We have reported on the detection of large-size ($\sim$360 kpc), faint (surface brightness 1.4−2.5 μJy arcsec^{-2}) radio jets in the nearby FR I (total luminosity $\sim 3.7 \times 10^{22}$ W Hz^{-1} at 144 MHz) elliptical galaxy NGC 5322 using the 144-MHz LoTSS DR2 image. Previously, the radio jets were detected only up to the $\sim$21 kpc extent in this galaxy. This detection highlights the unprecedented sensitivity achieved by the LOFAR in terms of detectable angular size at very low surface brightness. NGC 5322 is located in a region of the radio luminosity–size diagram where previously no radio galaxy of similar size has been reported within more than one order of magnitude luminosity. The low-density environment in terms of stellar core depletion, a lack of rich ISM in the galaxy and the low density of IGM surrounding the jets could be identified as the main cause of the long collimated jets, despite the low radio luminosity in NGC 5322. This result strengthens previous works where environments around the jets were found to be deciding factors for the observed radio morphologies. Some features of the jets, such as the abrupt dimming outside the optical extent of the galaxy and collimation on scales of 100 kpc in the IGM, are most intriguing.

A detailed study using multifrequency archival data from the GMRT and LOFAR is under way.

ACKNOWLEDGEMENTS

We thank the referee Heinz Andernach for constructive comments on the manuscript.

LOFAR data products were provided by the LOFAR Surveys Key Science project (LSKSP; https://lofar-surveys.org/) and were derived from observations with the International LOFAR Telescope (ILT). The efforts of the LSKSP have benefited from funding from the European Research Council, NOVA, NWO, CNRS-INSU, the SURF Co-operative, the UK Science and Technology Funding Council, and the Jülich Supercomputing Centre.

This research has made use of various on-line tools and data archives: the NASA Extragalactic Database, Skyview (https://skyview.gsfc.nasa.gov/), the Canadian Initiative for Radio Astronomy Data Analysis (CIRADA; http://cutouts.cirada.ca), cosmology calculators (https://cosmocalc.icrar.org), FIRST and NVSS data base from the US National Radio Astronomy Observatory, the SDSS data base provided by the Alfred P. Sloan Foundation, the US Department of Energy Office of Science, and the Participating Institutions, and the GMRT data provided by the National Centre for Radio Astrophysics of the Tata Institute of Fundamental Research (TIFR).

DATA AVAILABILITY

The images and data used in this paper are accessible from the open web-based archives of various radio and optical surveys, whose web links are provided in the acknowledgements.

REFERENCES

An T., Baan W. A., 2012, ApJ, 760, 77
Baldi R. D., Capetti A., 2009, A&A, 508, 603
Becker R. H., White R. L., Helfand D. J., 1995, ApJ, 450, 559

Capetti A. et al., 2022, A&A, 660, A93
Condon J. J., Cotton W. D., Greisen E. W., Yin Q. F., Perley R. A., Taylor G. B., Broderick J. J., 1998, AJ, 115, 1693
de Vaucouleurs G., de Vaucouleurs A., Corwin H. G. J., Buta R., Paturel G., Fouque P., 1991, Third Reference Catalogue of Bright Galaxies. Springer, Berlin
Dullo B. T. et al., 2018, MNRAS, 475, 4670
Fanaroff B. L., Riley J. M., 1974, MNRAS, 167, 31
Feretti L., Giovannini G., Hummel E., Kotanyi C. G., 1984, A&A, 137, 362
Finoguenov A., Davis D. S., Zimer M., Mulchaey J. S., 2006, ApJ, 646, 143
Gopal-Krishna, Wiita P. J., 2000, A&A, 363, 507
Gregory P. C., Condon J. J., 1991, ApJS, 75, 1011
Hardcastle M. J., Croston J. H., 2020, New Astron. Rev., 88, 101539
Hibbard J. E., Sansom A. E., 2003, AJ, 125, 667
Hummel E., 1980, A&AS, 41, 151
Hummel E., van der Hulst J. M., Dickey J. M., 1984, A&A, 134, 207
Intema H. T., Jagannathan P., Mooley K. P., Frail D. A., 2017, A&A, 598, A78
Kolokythas K., O'Sullivan E., Intema H., Raychaudhury S., Babul A., Giacintucci S., Gitti M., 2019, MNRAS, 489, 2488
Laing R. A., Bridle A. H., 2002, MNRAS, 336, 328
Lane W. M., Cotton W. D., van Velzen S., Clarke T. E., Kassim N. E., Helmboldt J. F., Lazio T. J. W., Cohen A. S., 2014, MNRAS, 440, 327
Makarov D., Karachentsev I., 2011, MNRAS, 412, 2498
Merloni A., Heinz S., di Matteo T., 2003, MNRAS, 345, 1057
Mingo B. et al., 2019, MNRAS, 488, 2701
Mulchaey J. S., Davis D. S., Mushotzky R. F., Burstein D., 2003, ApJS, 145, 39
Nagar N. M., Falcke H., Wilson A. S., 2005, A&A, 435, 521
Rengelink R. B., Tang Y., de Bruyn A. G., Miley G. K., Bremer M. N., Rottgering H. J. A., Bremer M. A. R., 1997, A&AS, 124, 259
Saikia D. J., 2022, preprint (arXiv:2206.05803)
Savini F. et al., 2017, MNRAS, 474, 5023
Serra P. et al., 2012, MNRAS, 422, 1835
Shimwell T. et al., 2022, A&A, 659, A1
Sramek R. A., 1975, AJ, 80, 771
Tonry J. L., Dressler A., Blakeslee J. P., Ajhar E. A., Fletcher A. B., Luppino G. A., Metzger M. R., Moore C. B., 2001, ApJ, 546, 681
van Haarlem M. P. et al., 2013, A&A, 556, A2
Velović V. et al., 2022, MNRAS, 516, 1865
Williams W. L. et al., 2019, A&A, 622, A2
Young L. M. et al., 2011, MNRAS, 414, 940

This paper has been typeset from a TEX/LATEX file prepared by the author.